ISSN: 0975-766X
Research Article
Available Online through
www.ijptonline.com

PHARMACOPHORE OPTIMIZATION OF SELECTIVE P38 MAP KINASE INHIBITORS AS POTENTIAL ANTI-INFLAMMATORY AGENTS USING MOLECULAR MODELING STUDIES

N. A. Khisti[a*], S.V. Gandhi[b]
Department of Pharmaceutical Chemistry, AISSMS College of Pharmacy, Near RTO, Kennedy Road, Pune-411001, India.
E-mail: nikhil_khisti@yahoo.co.in

Received on 25-03-2011 *Accepted on 10-04-2011*

Abstract

With the objective to design new chemical entities with enhanced inhibitory potencies against p38 MAP alpha kinase, the 2D, 3D-QSAR and Docking studies were carried out on Imidazothiazole compounds as inhibitors of these kinase is presented here. The developed model gave q^2 value of 0.5962 and r^2 value of 0.7375 for 2D QSAR while for 3D QSAR q^2 value of 0.8305 and Pred_r^2 value of 0.8170. The model is a useful tool for the prediction of test set of 4 compounds that were not included in the training set of 25 compounds. The results not only lead to better understanding of structural requirements of p38 alpha inhibitors but also can help in the design of new potent inhibitors. The binding mode of the compound at the active site of p38 MAP alpha kinase was explored using Glide docking program and hydrogen-bonding interactions were observed between the inhibitors and the target. The details of amino acid interactions of the active site are discussed briefly and correlated with the contour plots.

Key Words: MAP Kinase inhibitor, P38 MAP Kinase, Mitogen Activated protein kinase, 2D QSAR, 3D QSAR, Docking.

1. Introduction

p38 is a member of Ser/Thr kinases family [1] of the mitogen-activated protein (MAP) kinase super family [2,3]. The four-p38 isoforms, p38 α, p38 β, p38 γ, p38 δ varies based on their substrate specificity. The P38 α (also known as SAPK2 α, RK, CSBPs, Mxi2 or Mpk2) [4] and β are responsible for activation of heat shock proteins

Hsp 25, 27 and the MAPK activated protein MAPKAP-2 [5]. The actual activation of p38 occurs by dual phosphorylation of conserved Thr and Tyr residues [6] by upstream activators such as MAP kinase kinases (MKKs) upon receiving extra cellular signals [7]. The p38 MAP kinase regulates the release from leukocytes of IL-1 and TNF α, two cytokines that are associated with the progression of rheumatoid arthritis (RA) [8]. p38 is also implicated in the induction of COX-2, the inducible prostaglandin cyclo-oxiginase [9]. Inhibitors of the p38 α through their downstream blockage of the production of TNF α, IL- 1 β, IL-6, COX-2 and arachidonic acid mobilization have therapeutic potential [10,11]. These inhibitors not only block the synthesis but also the signal cascades induced by these cytokines [12] and prevent activation of caspases and apoptosis of neuronal cells and neuronal progenitor cells [13]. The interest in the development of p38 MAP kinase inhibitors is based on the expectations that p38 inhibiting drugs will treat the underlying cause of chronic inflammatory disease and cease their progression [14]. Although a number of structurally different inhibitors have been reported [15] to inhibit p38 with varying degrees of selectivity, none has reached commercial status [16]. Since, its introduction in last 2 decade of computer aided drug design techniques [17] has emerged as one of the most powerful tools. It includes structure based and ligand based drug design strategies [18]. The 2D and 3D QSAR methodology assumes that a suitable sampling of steric and electrostatic fields around a set of aligned molecules provides all the information necessary for understanding their biological properties [19]. The present study is aimed to gain insight into the steric and electrostatic properties of these compounds, their influence on the activity and to derive predictive 2D and 3D-QSAR models to design new class of inhibitors.

2. Material and Method

2.1. Biological data

Computational details:

All computational studies performed using V-Life sciences MDS Version 2.0. [20]. The compounds were constructed from the fragments in the V-life molecular Builder database with standard bond lengths and bond angles and geometry optimization was carried out using the standard Merck Molecular Force Field (MMFF) [21] with distance dependent-dielectric function and energy gradient of 0.001kcal/mol Å. The initial conformations selected and minimized using the Powell method until root-mean-square Deviation of 0.001 kcal/mol Å

obtained. Partial atomic charges calculated using the Gasteiger method. Further geometry optimization carried out for each compound with the MOPAC 6 package using the semi-empirical AM1 Hamiltonian. [22].

2.2. 2D-QSAR studies

Various descriptors were calculated and invariable columns removed. The 2D-QSAR performed using Partial least squares (PLS), Principle component regression (PCR) and Multiple Linear Regression (MLR) with simulated annealing (SA) as variable selection methods. Various 2D QSAR models were generated using, SA-PLS, SA-PCR and SA-MLR combinations. The SA-MLR resulted in best modeling and predictive efficiencies as compared to SA-PLS and SA-PCR.

2.3. 3D-QSAR kNN MFA

Template based method was done for alignment. Alignment of the compounds is a very important feature of 3D QSAR method and thus for kNN MFA analysis. For each alignment, the steric and electrostatic potential fields calculated for kNN-MFA at each lattice intersection of a regularly spaced grid box. The lattice spacing was set to a value of 2.0 Å in all X, Y and Z directions. Using a distance dependent dielectric constant of 1.0 A sp3 carbon atom with Van der Waals radius of 1.52 Å and + 1.0 charge was served as the probe atom to calculate steric and electrostatic fields.

2.3.1 Generation of 3D- QSAR models

Using standard kNN method in conjugation with the cross-validation (leave-one-out) option to determine the optimum number of components, which were then used in deriving the final 3D-QSAR model with cross-validation. The 3-D QSAR models using kNN MFA method were developed.

2.3.2. kNN-MFA with Simulated Annealing: - [23]

Simulated annealing (SA) is the simulation of a physical process, ‘annealing’, which involves heating the system to a high temperature and then gradually cooling it down to a preset temperature (e.g., room temperature). During this process, the system samples possible configurations distributed according to the Boltzmann distribution so that at equilibrium, low energy states are the most populated.

The SA kNN-MFA method employs the kNN classification principle combined with the SA variable selection procedure. For each predefined number of variables (Vn) it seeks to optimize using stochastic sampling and simulated annealing as an optimization tool.

(i) The number of nearest neighbors (k) used to estimate the activity of each molecule (ii) Using the selection of variables from the original pool of all molecular descriptors to calculate similarities between molecules (i.e., distances in Vn-dimensional descriptor space).

2.4. Design of new chemical entities using Lead grow tool [24]

The information obtained from 2D and 3D QSAR studies used to optimize the imidazothiazol nucleus for selective inhibition of the Integrase inhibitors. To ensure drug like pharmacokinetic profile of the designed NCEs, the following filters used while generating CombiLib,

A = Number of hydrogen Bond Acceptor (Not more than 8)

D = Number of Hydrogen Bond Donor are in range (Not more than 5)

R = Number of Rotatable Bond are in range (Not more than 10)

X = XlogP is in ideal range < 5

W=Molecular Weight is in ideal range < 500 Da

S= Polar surface area), (Not more than 60 Å2)

Dynamic Polar surface Area (PSAd) (S), (Not more than 60 Å2)

More than five hundred molecules generated by CombiLib tool of MDS using templet, which follows the Lipinski's rule. Compounds qualifying all required parameters set for Lipinski's screen filter are indicated by word ADRXWS, indicate that those requirements are satisfied by that corresponding compound. If molecules do not satisfy all six criteria, then those numbers of alphabet strings are missing from the column and the screen score reduced accordingly indicating lesser pharmacokinetic compatibility for that compound.

2.5. Docking studies

Molecular docking studies were performed using Glide (5.0) [25] molecular docking software. Selected most active molecules were docked on crystallographic structure of p38 MAP Kinase enzyme co-crystallized

with the ligand SB 20358 available in the RCSB PDB Database (Code: 1A9U) Molecular docking studies helps to determine possible interaction of NCEs with the enzyme on PDB(1A9U).

2.6 ADME Prediction

Prediction of the ADME parameter prior to the experimental studies is one of the most important aspects in the drug discovery and development of the drug molecule. Drug may fail to reach the market phase if those properties not fulfilled by the drug candidate. Taking into consideration the above-mentioned aspect, the ADME profile of the designed NCEs studied using QikProp 3.0 software [26].

QikProp is quick, accurate, eassy-to-use absorption, distribution, metabolism and excoriation (ADME) prediction program in Maestro, Schrodinger used here to predict ADME properties. QikProp predicts physically significant descriptors and pharmaceutically relevant properties of organic molecules, either individually or in batches.

3. Results and discussion

3.1 QSAR study

A series of total 29 compounds for which absolute IC_{50} values reported was [27] used for correlating chemical composition (structure) with their anti inflammatory activity.

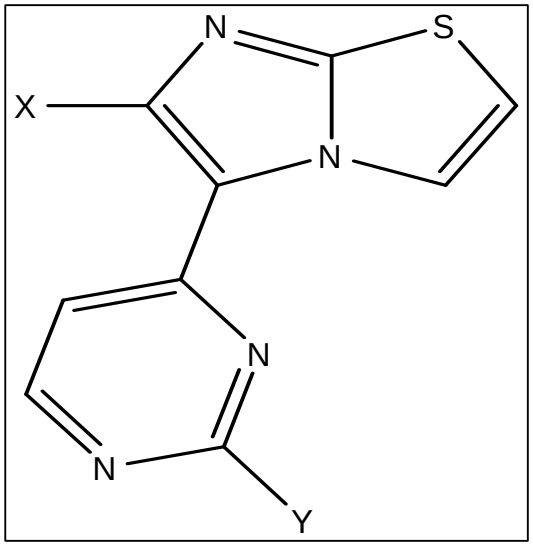

Fig. 1. Structure of imidazothiazole series showing sites for substitution.

Table 1: Structures of 2, 6 disubstituted-5-(2-substitutedpyrimidin-4-yl) imidazo [2, 1-b] thiazole derivatives.

Sr. No.	Comp. Name	X	Y
1.	**N 1**	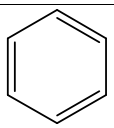	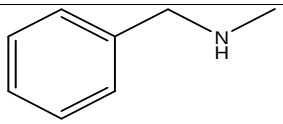
2	**N 2**	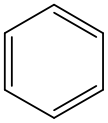	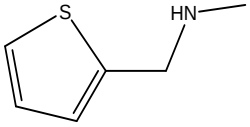
3.	**N 3**	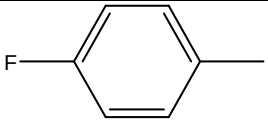	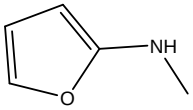
4.	**N 4**	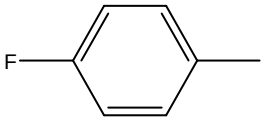	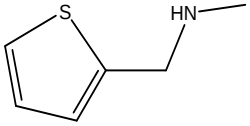
5.	**N 5**	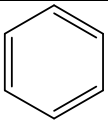	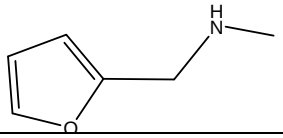
6.	**N 6**	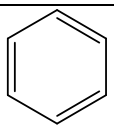	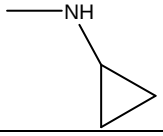
7.	**N 7**	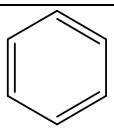	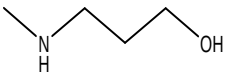
8.	**N 8**	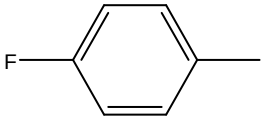	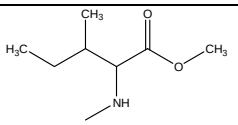
9.	**N 9**	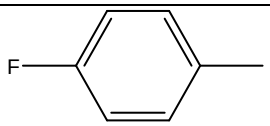	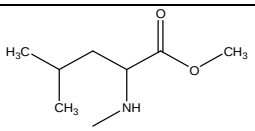
10.	**N 10**	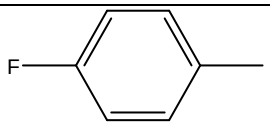	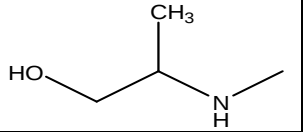

11.	**N 11**	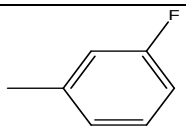	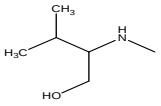
12.	**N 12**	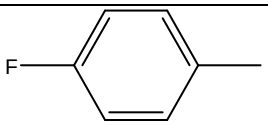	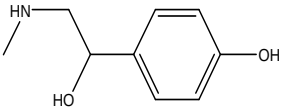
13.	**N 13**	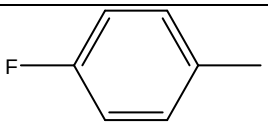	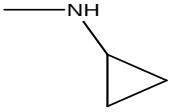
14.	**N 14**	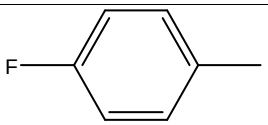	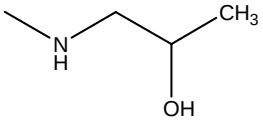
15.	**N 15**	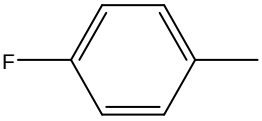	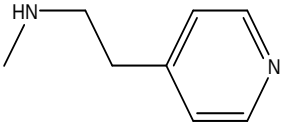
16.	**N 16**	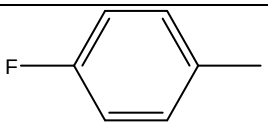	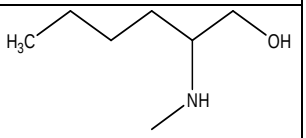
17.	**N 17**	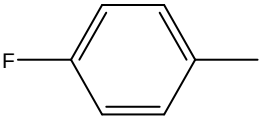	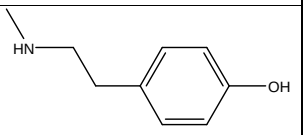
18.	**N 18**	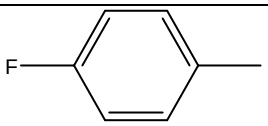	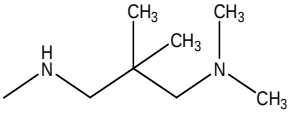
19.	**N 19**	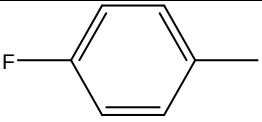	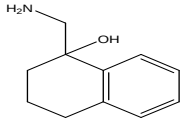
20.	**N 20**	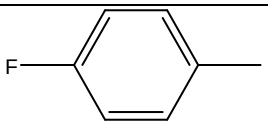	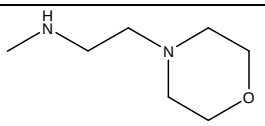
21.	**N 21**	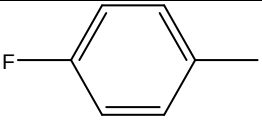	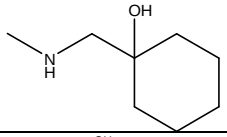
22.	**N 22**	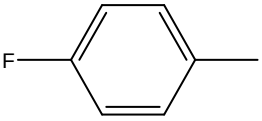	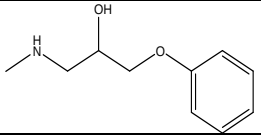
23.	**N 23**	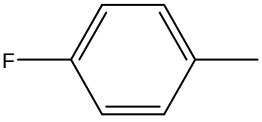	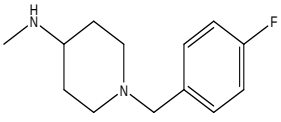

24.	**N 24**	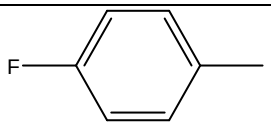	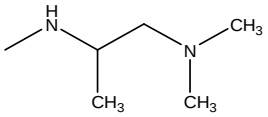
25.	**N 25**	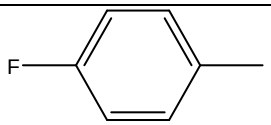	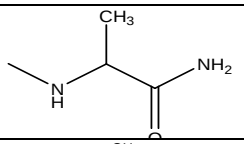
26.	**N 26**	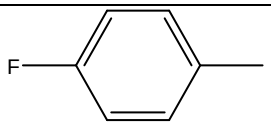	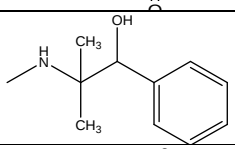
27.	**N 27**	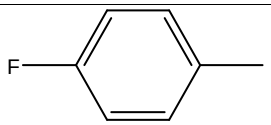	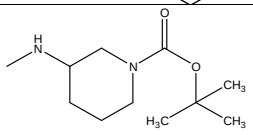
28.	**N 28**	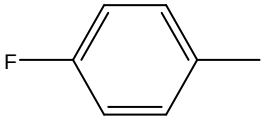	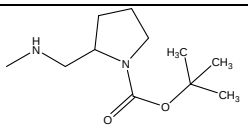
29.	**N 29**	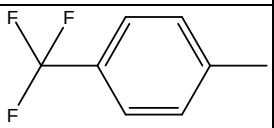	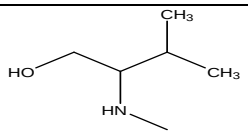

3.1.1 2D-QSAR studies

Various descriptors were calculated and invariable columns removed. The training and test sets divided into 25 and 4 compounds based on biological and chemical diversity. 2D-QSAR was performed using Partial least squares (PLS), Principle component regression (PCR) and Multiple regression regression (MLR) with simulated annealing (SA) as variable selection methods. SA- MLR resulted in best modeling and predictive efficiencies as compared to SA-PLS and SA-PCR. The obtained r^2 was 0.7375 with a q^2 of 0.5962 and predicted r^2 of 0.8150. The model equation given below (in Eq. 1) with statistical results of the 2D QSAR studied shown in (Table 2). Plot of observed versus predicted activities according to the model shown in equation-1 is shown in Fig 5.The best equation obtained, Equation No. 1, by 2D QSAR studies, showing contribution of different physicochemical parameters for Integrase selectivity is shown below.

pIC_{50} = 1.0145 (±0.1287) T_C_N_7 + 0.2173 (±0.0674) chi4-0.0482 (±0.0274) T_2_2_3 - 0.0609 (±0.0124) T_C_C_7 + 0.2209

(Eq. 1)

In Table 2, the statistical results for various statistical parameters along with the contribution of the descriptors for the 2D-QSAR model.

Table-2: Results of 2D QSAR.

Sr. no.	Statistical Parameter	Results	contributing Descriptors
1	Training Set Size (n)	25	
2	Test Set Size	4	
3	r^2	0.7375	
4	q^2	0.5962	T_2_2_3
5	Pred_r^2	0.8150	T_C_C_7
6	Pred_r^2 se	0.1804	T_C_N_7
7	F-Test	15.0191	chi4
8	Alpha Rand q2	2	
9	Best –Rand q2	2	
10	Z-score q2	2	

3.1.2 Evaluation of the 2D QSAR Models

The QSAR models were evaluated using following statistical measures

n - Number of molecules (data set should at least be ≥ 20 molecules).

Vn – Number of descriptors; also denoted by k.

K-Number of descriptors in a model (statistically n/5 descriptors in a model are preferred) (statistically 1 descriptor is selected for 5 compounds in the selected series of compounds n/5 number of descriptors are preferred).

df - degree of freedom (n-k-1) (higher is better).

r^2 - coefficient of determination (> 0.7 is better).

q^2 - cross validated r2 (>0.5 is better).

pred_r^2 - r^2 for external test set (>0.5 is better).

SEE- Standard Error of Estimate (smaller is better).

F-test- F-test for statistical significance of the model (higher is better, for same set of descriptors and molecules).

Table-3: Observed and predicted activities of the training and test set.

Comp. No.	Observed Value	Predicted Value	Residual Value
1	-0.76492	-1.04848	0.28356
2	-1.05691	-1.37476	0.31785
3	-0.92376	-1.16226	0.2385
4	-1.49969	-1.38835	-0.11134
5	-1.43457	-1.04329	-0.39128
6	-1.15534	-1.06952	-0.08582
7	-1.48001	-1.37548	-0.10453
8	-1.40483	-1.34961	-0.05522
9	-1.34635	-1.29959	-0.04676
10	-1.47712	-1.08816	-0.38896
11	-1.47422	-1.14321	-0.33101
12	-0.86094	-1.15208	0.29114
13	-2.96567	-2.97877	0.0131
14	-0.91487	-1.0204	0.10553
15	-0.78817	-1.0204	0.23223
16	-1.19313	-1.14491	-0.04822
17	-0.72346	-1.08507	0.36161
18	-1.33846	-1.07036	-0.2681
19	-1.45485	-1.15561	-0.29924
20	-1.12711	-1.07371	-0.0534
21	-1.1729	-1.0485	-0.1244
22	-0.79169	-0.96146	0.16977
23	-1.41497	-1.33641	-0.07856
24	-0.94498	-1.06093	0.11595
25	-1.12385	-0.96585	-0.158
26	-1.08279	-0.95589	-0.1269
27	-0.76864	-1.04411	0.27547
28	-0.7364	-0.98347	0.24707
29	-1.0086	-1.14491	0.13631

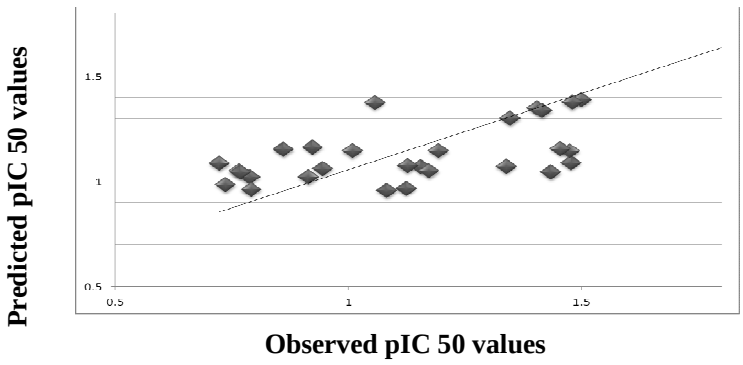

Fig. 2 Observed versus predicted activities of Training and Test set according to the model shown in Eq.1

3.2. 3D-QSAR studies

All the optimized compounds aligned using the template based alignment method. The template taken for the alignment is shown in fig.3(a). Topological, steric and electrostatic descriptors were calculated. The 3D-QSAR studies performed using kNN- MFA that adopts the k-Nearest Neighbor principle. KNN-MFA generates relationships between molecular field and biological activity. The 3D QSAR models generated using SA-kNN. In this method, an unknown member classified according to the majority of its k-Nearest Neighbors in the training set.

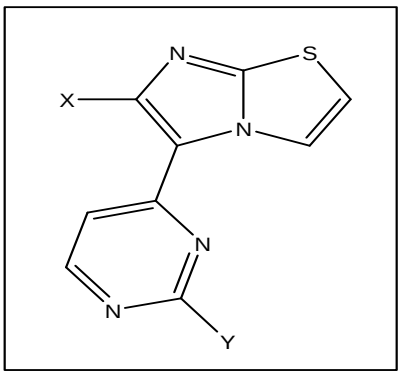

Fig.3 (a) Common template used for alignment.

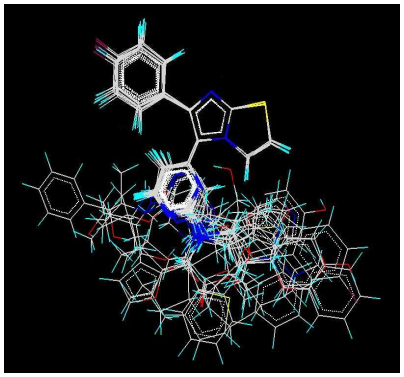

(b) Alignment of Substituted Imidazothiazole derivatives using template based alignment method.

Table 5: Comparison of the various statistical results of 3D QSAR generated by SA kNN- MFA Methods.

Parameter	SIMULATED ANNEALING kNN -MFA	STEP WISE kNN –MFA
q^2	0.7231	0.8305
q^2_se	0.2231	0.2489
Pred_r^2	0.7005	0.8170
Pred_r^2_se	0.1607	0.3206
Contributing descriptors		
Hydrophobic	---	H_388 (0.3101, 0.3328)

Electrostatic	E_592 (0.3296 , 0.3997) E_132 (-0.0123 , 0.0745) E_1623 (0.3302, 0.4333)	E_813 (-0.2104, 0.0120) E_211 (0.0412, 0.0843)
Steric	S_500 (-0.0110, -0.0055)	S_605 (-0.5261, -0.4538) S_753 (-0.0553, -0.0439) S_151 (-0.0007, -0.0004)

The model obtained from SA kNN MFA show best internal as well as external predictivity (q^2 = 0.7231, pred_r^2 = 0.7005) also The SE internal & external validation was very low (q^2_se = 0.2231, pred_r^2_se = 0.1607) as compared to other models resultant Eqs are shown in Eq.2. The 3D data points generated around rectangular grid along with range of contribution of steric & electrostatic data points are mentioned in parenthesis using SA kNN-MFA model are depicted in (Fig-4).

Thus SA kNN MFA model was used to optimize the electronic as well as steric requirement around pharmacophore.

pIC_{50}= -0.0110 S_500 + 0.3296 E_592 + 0.3302 E_1623 -0.0123 E_132 (Eq. 2).

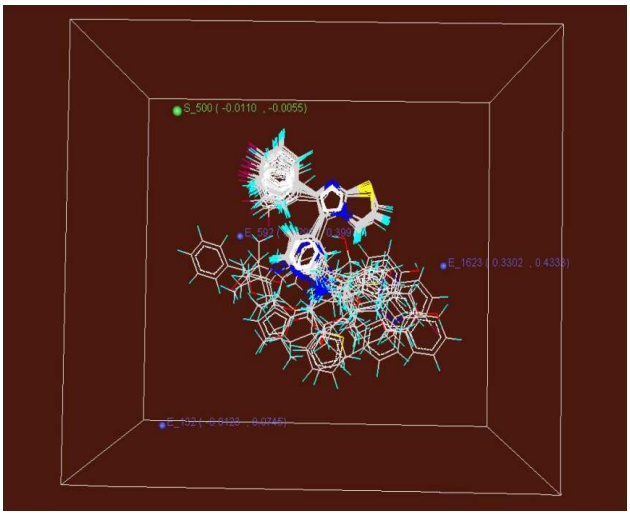

Fig.4 Stereo view of the molecular rectangular field grid around the superposed molecular units of Imidazothiazole series of compounds by using SA kNN MFA Method.

3.2.1 kNN-MFA interaction energies

For each alignment, the steric and electrostatic potential fields for kNN-MFA calculated at each lattice intersection of a regularly spaced grid box. The lattice spacing was set to a value of 2.0 Å in all X, Y and Z

directions. A distance –dependent dielectric constant of 1.0 was used. A sp3 carbon atom with Van der Waals radius of 1.52 Å and + 1.0 charge was served as the probe atom to calculate steric and electrostatic fields.

3.3 Interpretation of QSAR Studies

It is simple to interpret a 2D QSAR MLR equation where each descriptor's contribution seen by the magnitude and sign of its regression coefficient. A descriptor's coefficient magnitude shows its relative contribution with respect to other descriptors and sign indicates whether it is directly (+) or inversely (-) proportional to the activity. The developed MLR Equation1 indicated that **T_2_2_3** alignment independent (AI) descriptors class**.** This is the count of number of double bounded atoms (i.e. any double bonded atom, T_2) separated from any other double bonded atom by 3 bonds in a molecule. **T_C_N_7** this is the count of number of nitrogen atoms (single, double or triple bonded) separated by any other carbon atom. **Chi4,** which is directly proportional to the activity and shows the role of atomic valence connectivity index (order 4). **T_C_C_7** this is the count of number of two carbon atoms separated from each other's by 7 bonds, which contributes negatively.

3D QSAR was used to optimize the electrostatic and steric requirements around carboxamide pharmacophore. 3D data points were generated which contribute to SA kNN MFA (Fig.4). The range of property values for the generated data points helped for the design of potent NCEs. The range was based on the variation of the field values at the chosen points using the most active molecule and its nearest neighbor set. The points generated in SA KNN MFA 3D QSAR model are E_592 (0.3296 , 0.3997) E_132 (-0.0123, 0.0745) E_1623 (0.3302, 0.4333) S_500 (-0.0110, -0.0055) i.e. Steric, & electrostatic interaction field at lattice points 500, 592, 132 and 1623 respectively.

These points were suggested the significance and requirement of steric, & electrostatic properties as mentioned in the ranges in parenthesis for structure activity relationship and maximum biological activity of imidazothiazole derivatives.

Negative and positive values in electrostatic field descriptors indicated the requirement of negative and positive electrostatic potential respectively for enhancing the biological activity of imidazothiazole derivatives.

Blue contours are observed near pyrimidine ring which indicates importance of electropositive substituents at this position. Blue counter around pyrimidine substituted groups indicates importance of

electronegative group in plane. Yellow contours are observed around substituted phenyl group indicate sterically unfavorable position for substitution.

3.4. Design of New Chemical Entities (NCEs) Containing Imidazothiazole pharmacophore for selective inhibition of p38 MAP Kinase enzyme.

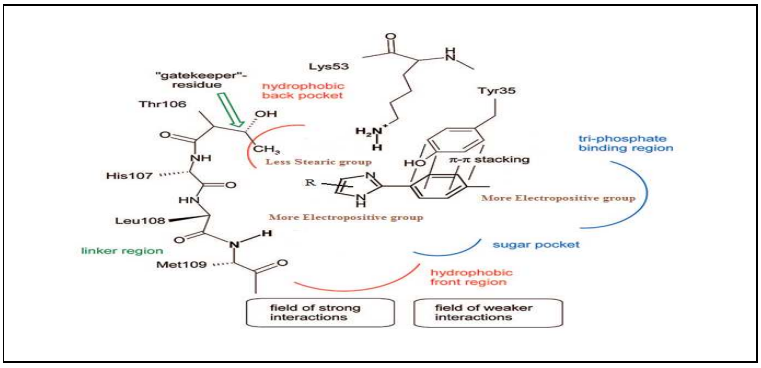

The information obtained from 2D and 3D QSAR studies was used to optimize the electrostatic, hydrophobic and steric potentials requirement around the selected common template of imidazothiazole for inhibition of p38 MAP Kinase enzyme. According to the literature survey and data obtained from QSAR, docking studies it comes to know that nitrogen containing Heterocyclic ring is essential for activity therefore we did not made any change in this group.

- Important findings for selective inhibitor of p38 α MAP Kinase.

1) Hydrogen donor/acceptor function group containing ring residues within the hinge region (mainly gaining activity);

2) Space-filling lipophilic aromatic residues binding to the hydrophobic back pocket (also hydrophobic region I, mainly gaining selectivity);

3) Interactions with the hydrophobic front region (also hydrophobic region II, Figure 3.4, gaining both activity and selectivity);

4) Further interactions with both the sugar pocket and the phosphate binding region (importance less clear, preferred positions to modify physicochemical properties).

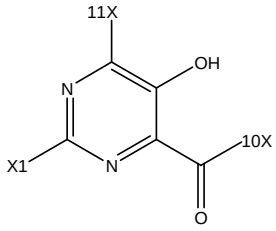

NIK SERIES

Common template used for the design of NCEs.

Table No-6: List of Compounds designed through CombiLib Approach using Regression equation Obtained by 2-D QSAR studies along with predicted activities.

Sr. No	Molecule No.	1x	10x	11x	Predicted activity	Screen result	Screen score
1	NIK 1	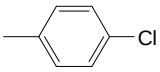	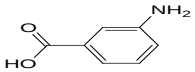	-OH	-1.70594	ADRXWS	6
2	NIK 2	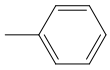	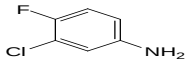	-OH	-1.69032	ADRXWS	6
3	NIK 3	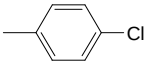	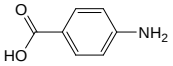	-OH	-1.71496	ADRXWS	6
4	NIK 4	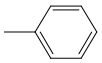	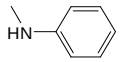	-OH	-1.73059	ADRXWS	6
5	NIK 5	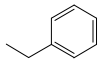	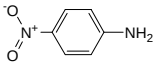	-OH	-1.73035	ADRXWS	6
6	NIK 6	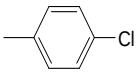	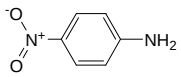	-OH	-1.71472	ADRXWS	6
7	NIK 7	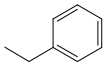	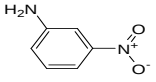	-OH	-4.26429	ADRXWS	6
8	NIK 8	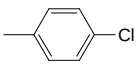	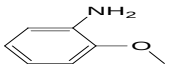	-OH	-1.6971	ADRXWS	6
9	NIK 9	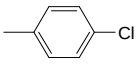	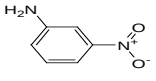	-OH	-4.24866	ADRXWS	6
10	NIK 10	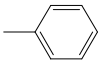	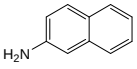	-OH	-1.65912	ADRXWS	6

3.5 Molecular modeling studies.

To cross verify the results obtained by 2D and 3D QSAR studies (Dry Lab Work) and results obtained by synthetic and pharmacological work (Wet Lab Work) docking is carried out on Pdb (Code: 1A9U).

Table No-7: Results of Extra precision docking studies of 5, 6-Dihydroxy pyrimidine Series of compounds along with standard p38 MAP Kinase inhibitors.

Sr. No.	Title	G-Score	Energy	Hbnd	Good vdw	Bad vdw	Ugly vdw
1	NIK 5 N	-7.48	-61.7	3	225	1	1
2	NIK 5 J	-7.11	-46.6	4	207	3	3
3	NIK 4G	-6.83	-40.1	1	299	1	0
4	NIK 3N	-6.73	-42.8	3	192	5	1
5	**SB20358**	-6.72	-43.0	3	278	5	1
6	NIK 4Q	-6.50	-38.7	3	228	4	2
7	**RMJ 67657**	-6.42	-46.2	2	274	6	2
8	NIK 5 H	-6.45	-43.5	3	243	2	2
9	NIK 5 B	-6.43	-42	4	199	6	2
10	NIK 5 K	-6.43	-45.5	4	210	5	1
11	NIK 5 P	-6.42	-44	3	229	5	0
12	NIK 5 S	-6.35	-40.9	3	198	4	0
13	NIK 4 W	-6.32	-43.3	2	256	4	1
14	NIK 4 L	-6.13	-43.6	3	269	3	1
15	NIK 3 Q	-6.29	-36.7	3	224	8	2
16	NIK 5 C	-6.25	-41.8	4	207	7	2
17	NIK 3 B	-6.20	-41.2	3	169	6	1
18	NIK 4 K	-6.16	-39.8	2	169	1	1
19	NIK 4 T	-6.13	-41.3	4	137	5	1
20	NIK 4F	-4.47	-36.6	1	193	5	0
21	NIK5W	-4.49	-47.8	1	231	2	0
22	NIK 5F	-4.59	-36.9	2	173	1	0
23	NIK 4D	-.4.45	-37	1	221	5	0
24	NIK 5T	-4.51	-38	1	208	2	0
25	NIK 5V	-4.49	-36.4	1	231	2	0

Hbond = No. of Hydrogen bonds. Bad vdw = No. of Bad Van Der Waals Contacts. Ugly vdw = No. of Ugly Van Der Waals Contacts.

The reliability of the docking results was first evaluated by comparing the best docking poses obtained for the co-crystallized inhibitor with its bound conformation. As a result, a root mean square deviation (RMSD) of 0.7 Å was found, and it suggested that the docking procedure could be relied on to predict the binding mode of our compounds. The docking results were evaluated based on Glide Score (G Score), Hydrogen bonds (H-bond) and Vander Waals (VDW) Interaction between ligands and receptor.

3.5.1 Docking results

The close inspection of result of molecular docking studies indicated that the designed compounds docked better than CO-crystallize ligand SB 20358.

Following are the reasons for the same.

- Number of required H-bond are significantly higher i.e. 4 to 2 in top compounds in docking results table as compared to SB 20358 which forms 3 bond.
- The number of good wander wals interaction are also significant ranging 299 to 192 in top scoring compounds as compared to SB 20358 which form 278 good wander waals interaction.
- Number of bad Van der walls interactions range from 1 to 5 in top scoring compounds as compared to SB 20358 which forms 5 bad Van der walls interactions.
- The number of ugly Van der walls interactions lies in range 0 to 3 in in top scoring compounds as compared to SB 20358 that also forms only 1 ugly Van der walls interactions.

4. Conclusion

In an attempt to identify new and potent p38 MAP kinase inhibitors, we tried to generate simplest hypothesis that could correctly predict the activity of compounds belonging to the Imidazole class. The 3D QSAR hypotheses obtained should give important guidance for the design of novel p38 MAP kinase inhibitors.

The thorough analysis of results of 2D and 3D QSAR studies have helped us to make a decision about the electronic, steric, hydrophobic and topological nature of substitution pattern around the selected pharmacophore.

Using the information the New Chemical Entities (NCEs) were designed using CombiLib tool with the help of 2D QSAR regression equation and activities were also computed for the designed NCEs.

Designed compounds were screened by three types of screening methods for finding of new compounds with anti inflammatory activity, (i) Lipinski's rule and prediction of activity using regression equation generated by 2D QSAR studies, (ii) Docking studies and (iii) Prediction of ADMET properties. Three compounds were selected from results of molecular modeling studies and were synthesized.

The generated NCEs using combiLib was analyzed by Lipinski's screen. Results indicated that designed NCEs are satisfying all the parameters set for Lipinski's screen. The most potent derivatives were subjected to molecular docking studies to get further insights of interactions of NCEs with Integrase. Finally top 3 compounds with good docking score will be subjected to wet lab work viz., synthesis and evaluation of Integrase inhibitory assay studies.

The results of dry lab work and wet lab work will be analyzed thoroughly to find out correctness of the rational used for the design of NCEs in general and optimization of pharmacophore for selective inhibition of p38 MAP Kinase in particular.

5. Acknowledgement

Authors are very much thankful to Prof. S.V.Gandhi for blessing us with detailed insights of molecular modeling studies. Authors are also thankful to Dr. A. R. Madgulkar, Principal of our institute for continuous motivation, support and for providing the necessary infrastructure to carry out this work.

6. References

1. P. Sandra, J.P. Maria, M.C. Pedro, S.M. Victoria, R.G. Ana, C. Piero, M. Federico Jr., M. Cristina, Curr. Biol. 16 (2006) 2042-2047.
2. J.C. Lee, J.T. Laydon, P.C. McDonnell, T.F. Gallagher, S. Kumar, D. Green, D. McNulty, M.J. Blumenthal, J.R. Heys, S.W. Landvatter, J.E. Stricker, M.M. McLaughlin, J.R. Siemens, S.M. Fisher, G.P. Livi, J.R. White, J.L. Adams, P.R. Young, Nature 372 (1994) 739.
3. J. Hans, J.-D. Lee, L. Bibbs, R.J. Ulevitch, Science 265 (1994) 808.
4. B.L. Rachel, H. Steven, W. Rebecca, F.P. Hugh, J.M. Christopher, Curr. Biol. 8 (1998) 1049-1057.

5. J.C. Kyra, B.S. Kenneth, J. Exp. Biol. 206 (2003) 107.
6. J.B. Alastair, K. Stefan, Trends Pharmacol, Sci. 27 (2006) 525-530.
7. A.M. Badger, J. Bradbeer, B. Votta, J.C. Lee, J.L. Adams, D.E. Griswals, J. Pharm. Exp. Ther 279 (1996) 1453.
8. A.H. Julianne, K. Florida, D.R. Rowena, J.S. Peter, Ida Ita, X.M. Sherrie, V.P. James, E.C.A. Cornelis Hop, K. Sanjeev, W. Zhen, J.O. Stephen, A.O. Edward, P. Gene, E.T. James, W. Andrew, M.Z. Dennis, B.D. James, Bioorg. Med. Chem. Lett. 13 (2003) 467.
9. J.C. Lee, M.J. Blumenthal, J.T. Laydon, K.B. Tan, D.L. DeWitt,W.W. Lin, B.C. Chen, J. Pharmacol. 126 (1999) 1419.
10. A.D. Mark, A.L. Michael, F.M.C. Kim, T.B. John, J.C. Thomas, R.C. Santo, C. Csilla, J.D. Alan, C.E. Nancy, A.G. Christopher, K.J. Crystal, M.L. Jeff, H.M. William, M.P. Kevin, A.S. Ingrid, S. Linne, J.S. Francis, H.Y. Chul, Bioorg. Med. Chem. Lett. 14 (2004) 919-923.
11. J.L.Adams,A.M.Badger, S.Kumar, J.C.Lee, Prog.Med.Chem. 38 (2001) 1.
12. S. Kumar, P.C. McDonnell, R.J. Gum, A.T. Hand, J.C. Lee, P.R. Young, Biochem. Biophys. Res. Commun. 235 (1997) 533.
13. J. Harada, M. Sugimoto, Jpn. J. Pharmacol. 79 (1999) 369-378.
14. R. Laszlo, E.D. Franco, B. Thomas, F. Roland, G. Hermann, H. Pete, M. Ute, W. Romain, G.Z. Alfred, Bioorg. Med. Chem. Lett. 12 (2002) 2109.
15. (a)C. Dominguez, D.A. Powers, N. Tamayo, Curr. Opin. Drug. Disc. 8 (2005) 421;
    (b)D.M. Goldstein, T. Gabriel, Curr. Top. Med. Chem. 10 (2005) 1017.
16. (a)J. Hynes, K. Leftheris, Curr. Top. Med. Chem. 10 (2005) 967;
    (b)F.G. Salituro, R.A. Germann, K.P. Wilson, G.W. Bemis, T. Fox, M.S.-S. Su, Curr. Med. Chem. 6 (1999) 807.
17. R.D. Cramer III, D.E. Patterson, J.D. Bunce, J. Am. Chem. Soc. 110(1998) 5959-5967.
18. G.R. Desiraju, B. Gopalakrishnan, R.K. Jetti, A. Nagaraju, J.D. Raveendra, A. Sharma, M.E. Sobhia, R. Thilagavathi, J. Med. Chem. 45 (2002) 4847-4857.

19. S.K. Singh, N. Dessalew, P.V. Bharatam, Eur. J. Med. Chem. 41 (2006), 1310-1319.

20. VLIfeMDS, Molecular Design Suit Version 2.0, V–Life Science TechnologiesPvt.LTD. Pune, India, 2004.

21. T. A. Halgren, Merck Molecular Force Field. III. Molecular Geometries and. Vibrational Frequencies, J. Comp. Chem. 17 (1996) 520–552.

22. K.Ohtawara and H.Teramae, Study on optimization of molecular structure using Hamiltonian algorithm, Chemical physics Letters, 390 (2004) 84-88.

23. S. Ajmani, K. Jadhav, and S. Kulkarni,Three-Dimensional QSAR Using the k-Nearest Neighbo Method and Its Interpretation, J. Comp. Inf. & Model,46 (2006) 24–31.

24. C. A. Lipinski, F. B. Lombardo, W. Dominy and P. J. Feeney, Experimental and computational approaches to estimate solubility and permeability in drug discovery and development settings Adv. Drug. Deliv. Rev., (1997) 23-25.

25. Glide, Molecular Docking Tool of Schrodinger Inc., Version 5.0, New York, USA.

26. QikProp, Version 3.1, Schrodinger LLC, New York.

27. Alessia Petrocchi et al., From dihydroxypyrimidine carboxylic acids to carboxamide HIV-1 integrase inhibitors; SAR around the amide moiety, B.M.C.Letters 17 (2007) 350-353.

Corresponding Author:

N. A. Khisti[a*],

AISSMS College of Pharmacy,

Near RTO, Kennedy Road,

Pune-411001, Maharashtra, India.

Email: *nikhil_khisti@yahoo.co.in*